

## B<sub>1</sub>-control Loop Array for Reduction of B<sub>1</sub> Inhomogeneity

Y. Kaneko<sup>1</sup>, H. Habara<sup>1</sup>, Y. Soutome<sup>1</sup>, H. Ochi<sup>1</sup>, and Y. Bito<sup>1</sup>

<sup>1</sup>Central Research Laboratory, Hitachi Ltd., Kokubunji-shi, Tokyo, Japan

### INTRODUCTION

The inhomogeneity of B<sub>1</sub> in a human body increases as the strength of a static magnetic field increases and the RF wavelength becomes shorter. Various methods have recently been developed to reduce the inhomogeneity, such as dielectric pads [1,2], coupling coils [3-6] and RF shimming. However, B<sub>1</sub> inhomogeneity still remains in some cases of abdominal imaging, and a more effective method for reducing B<sub>1</sub> inhomogeneity is required. Our previous study showed that using the 'B<sub>1</sub> rectifying fin' can control the B<sub>1</sub> field locally and reduce B<sub>1</sub> inhomogeneity [7]. In order to combine the B<sub>1</sub> homogenization function of the fin with receive array coils, we're changing the shape of the fin into a loop. In this study, we have proposed a new method of B<sub>1</sub> homogenization: using a 'B<sub>1</sub>-control loop array' combined with RF shimming. This method improves B<sub>1</sub> homogeneity more than using RF shimming alone does.

### METHOD

**Design:** The magnetic flux around the conductive fin and loop is illustrated in Figure 1. As shown in Fig. 1(a), the fin can change the magnetic flux because of an electrical counter current flow. The loop, which has sufficiently lower resonance frequency than the transmit RF frequency, exhibits inductive characteristics. The inductive loop changes the flux in the same direction as the fin in Fig. 1(b). The flux density becomes lower around the center of the loop and higher near the edge of the loop. The spatial distribution of the flux density around the loop has a potential to compensate the B<sub>1</sub> inhomogeneity. The loop array is arranged around the abdomen with the some loops used as 'on-mode' and the others used as 'off-mode'. The on-mode means a loop with no capacitor or additional inductor, and the loop works as shown in Fig. 1(b). The off-mode means a loop with some electric cutting point, and the cut-loop can pass the flux. The loop array compensates the B<sub>1</sub> inhomogeneity by selecting the modes, considering the position of larger and smaller B<sub>1</sub> regions in the abdomen. **Simulation:** The effect of the B<sub>1</sub>-control loop array was clarified with numerical analysis of the B<sub>1</sub> field, using an electromagnetic simulation tool (xFDTD<sup>TM</sup>). The simulation model of the loop array is shown in Figure 2. A 2-channel birdcage coil was used for RF transmission, and the RF frequency was 128 MHz. The phantom size was 350 x 200 mm (x-y plane). The conductivity and relative permittivity of the phantom were 0.6 S/m and 80, respectively. Twelve loops were arranged around the phantom, and each loop size was 120 x 250 mm. Six loops were used in on-mode (No. 1, 4, 5, 8, 9 and 12), and the others were used in off-mode, considering the optimal modes based on the previous study [7]. The value of B<sub>1</sub> homogeneity (U<sub>SD</sub>) was defined as  $U_{SD} = \sigma / \bar{B}_1$ , where  $\sigma$  is the standard deviation of B<sub>1</sub>, and  $\bar{B}_1$  is the average of B<sub>1</sub>. **Experiment:** Phantom imaging was done with a 3T MR scanner (Varian INOVA). The setup of the B<sub>1</sub>-control loop array is shown in Figure 3. Twelve loops are made of copper tape, and each loop size was 120 x 240 mm. The phantom size was 310 x 220 mm. B<sub>1</sub> map was accomplished using the double-angle method. The sequence parameters were as follows: FOV = 450 mm, TR/TE = 1500/8.5 ms, matrix = 64 x 64, thickness = 10 mm and flip angle = 60, 120 degrees.

### RESULTS AND DISCUSSION

The simulation results of the B<sub>1</sub> field in the phantom are shown in Figure 4. Case (a) represents the phantom without loop array in quadrature drive (QD) mode, and case (b) represents that in RF shimming mode, case (c) represents the phantom with loop array in QD mode, and case (d) represents that in RF shimming mode. The B<sub>1</sub> values were normalized with the average of B<sub>1</sub> in case (a). The B<sub>1</sub> map was the most homogeneous in case (d), in which both the B<sub>1</sub>-control loop array and RF shimming were used. The B<sub>1</sub> homogeneity value (U<sub>SD</sub>) for (a), (b), (c) and (d) were 0.321, 0.256, 0.277 and 0.222, respectively. U<sub>SD</sub> decreases in the case (d), comparing U<sub>SD</sub> in other cases. The experimental results of B<sub>1</sub> map in the phantom are shown in Figure 5. The values of U<sub>SD</sub> for (a), (b), (c) and (d) were 0.367, 0.297, 0.316 and 0.269, respectively. The B<sub>1</sub>-control loop array reduces B<sub>1</sub> inhomogeneity, and the tendency was the same as the simulation results. The averages of B<sub>1</sub> in all cases (a), (b), (c) and (d) were also calculated, and they were almost the same. We found that B<sub>1</sub>-control loop array can improve B<sub>1</sub> homogeneity, maintaining the average of B<sub>1</sub>.

### CONCLUSION

We have proposed a new method of B<sub>1</sub> homogenization: using a B<sub>1</sub>-control loop array combined with RF shimming. The results of both FDTD simulation and experiments show that the B<sub>1</sub>-control loop array, used with RF shimming, was more effective in reducing B<sub>1</sub> inhomogeneity than RF shimming alone.

### REFERENCES

- [1] Schmitt M et al. ISMRM 2004; 11: 197.
- [2] Kendra MF et al. J Magn Reson Imaging 2008; 27: 1443-1447.
- [3] Schmitt M et al. ISMRM 2005; 13: 331.
- [4] Wang S et al. ISMRM 2007; 15: 3275.
- [5] Sacolick L et al. ISMRM 2010; 18: 3809.
- [6] Hancu I et al. ISMRM 2010; 18: 2470.
- [7] Kaneko Y, et al. ISMRM 2010; 18: 3810.

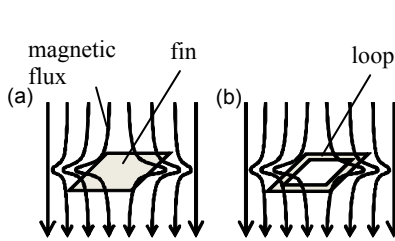


Figure 1 Magnetic flux around (a) conductive fin and (b) loop.

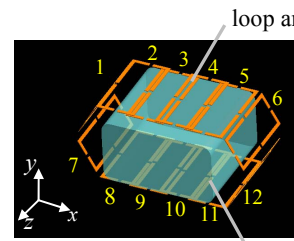


Figure 2 Simulation model of B<sub>1</sub>-control loop array.



Figure 3 Experimental setup of B<sub>1</sub>-control loop array.

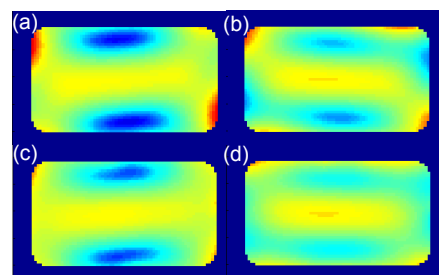


Figure 4 Simulation results with phantom. B<sub>1</sub> map for (a) QD alone, (b) RF shimming alone, (c) QD with loop array, and (d) RF shimming with loop array.

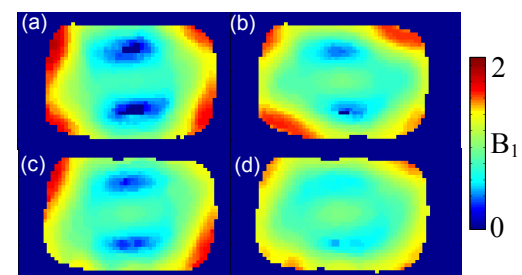


Figure 5 Experimental results with human abdomen. B<sub>1</sub> map for (a) QD alone, (b) RF shimming alone, (c) QD with loop array, and (d) RF shimming with loop array.